

Experimental investigation of dynamical invariants in bipartite entanglement

O. Jiménez Farías*, A. Valdés Hernández, G. H. Aguilar, P. H. Souto Ribeiro†, S. P. Walborn, and L. Davidovich
*Instituto de Física, Universidade Federal do Rio de Janeiro,
 Caixa Postal 68528, Rio de Janeiro, RJ 21941-972, Brazil*

Xiao-Feng Qian and J. H. Eberly

Rochester Theory Center and the Department of Physics & Astronomy, University of Rochester, Rochester, New York 14627

(Dated: November 14, 2018)

The non-conservation of entanglement, when two or more particles interact, sets it apart from other dynamical quantities like energy and momentum. It does not allow the interpretation of the subtle dynamics of entanglement as a flow of this quantity between the constituents of the system. Here we show that adding a third party to a two-particle system may lead to a conservation law that relates the quantities characterizing the bipartite entanglement between each of the parties and the other two. We provide an experimental demonstration of this idea using entangled photons, and generalize it to N-partite GHZ states.

Introduction. Proper understanding of the production, quantification and evolution of quantum entanglement has been a major challenge of quantum physics, with direct implications on the relevance of this resource for applications in quantum information. A particularly important problem concerns the decay of initially entangled states under the influence of independent reservoirs acting on each part of the system. While each of these parts undergoes a typical decoherence process, affecting the populations and the coherences of the state, the dynamics of entanglement may differ considerably from local dynamics [1–15].

Usually, entanglement is not a conserved quantity. For instance, when an initially excited atom decays, releasing a photon into a zero-temperature environment, the initial and final states of the atom-environment system are not entangled, but the atom does get entangled to the environment at intermediate times. We show nevertheless that adding a third party to this two-party system leads to a conservation law involving quantities that measure the bipartite entanglement between each part of the system and the other two parts. The introduction of this external party unveils therefore a hidden conservation law for entanglement. We demonstrate it experimentally using twin photons, which have been useful tools for exploring subtle properties of quantum physics and quantum information [16]. We follow here the strategy of [11, 14], which allows one to study the detailed dynamics of entangled states with optical interferometers. We also point out a generalization of this conservation law to N-partite GHZ states.

Invariants in two-qubit dynamics. Let S be a qubit and R the reservoir with which it interacts after $t = 0$. The initial product state of the S - R system is assumed to be

$$\rho_{SR}(0) = \rho_S(0) \otimes \rho_R(0), \quad (1)$$

with

$$\rho_S(0) = \begin{pmatrix} \rho_{gg} & \rho_{ge} \\ \rho_{eg} & \rho_{ee} \end{pmatrix}, \quad \rho_R(0) = |\phi_0\rangle \langle \phi_0|. \quad (2)$$

The matrix ρ_S is written in the basis $\{|g\rangle, |e\rangle\}$ of the ground and excited states of S , and $|\phi_0\rangle$ stands for the ground state of the reservoir R . At $t = 0$ both S and R start to interact in such a way that the following transformation holds:

$$\begin{aligned} |g\rangle |\phi_0\rangle &\rightarrow |g\rangle |\phi_0\rangle, \\ |e\rangle |\phi_0\rangle &\rightarrow \sqrt{1-p} |e\rangle |\phi_0\rangle + \sqrt{p} |g\rangle |\phi_1\rangle, \end{aligned} \quad (3)$$

where $p = p(t) \in [0, 1]$ is a time-dependent parameter such that $p(0) = 0$, $p(\infty) = 1$, and $|\phi_1\rangle$ denotes the first excited state (orthogonal to $|\phi_0\rangle$) of R . The map (3) corresponds precisely to the amplitude damping channel. For different parameterizations $p(t)$, the transformation (3) represents several physical processes such as the spontaneous emission of a photon by a two-level atom in a zero-temperature electromagnetic environment, or the interaction of a two-level atom with a single mode of the electromagnetic field inside a cavity. According to the map (3), the matrices (2) evolve into:

$$\begin{aligned} \rho_S(p) &= \begin{pmatrix} 1 - \rho_{ee}(1-p) & \rho_{ge}\sqrt{1-p} \\ \rho_{eg}\sqrt{1-p} & \rho_{ee}(1-p) \end{pmatrix}, \\ \rho_R(p) &= \begin{pmatrix} 1 - \rho_{ee}p & \rho_{ge}\sqrt{p} & \dots \\ \rho_{eg}\sqrt{p} & \rho_{ee}p & \dots \\ \dots & \dots & \dots \end{pmatrix}, \end{aligned} \quad (4)$$

where “...” in the expression for $\rho_R(p)$ represents empty rows and columns corresponding to the infinite remaining null matrix elements. Inspection of the reduced density matrices (4) shows that the information initially contained in the system S is transferred to the system R . The transfer is complete at $p = 1$, when the states of S and R become exchanged.

An important observation regarding the dynamics imposed by the transformation (3) is that the mean number $\langle \hat{N} \rangle$ of total excitations,

$$\langle \hat{N} \rangle = \langle \hat{n}_S(p) + \hat{n}_R(p) \rangle, \quad (5)$$

*Also with Instituto de Ciencias Nucleares, Universidad Nacional Autónoma de México (UNAM), Apdo. Postal 70-543, México 04510 D.F.

†Corresponding author e-mail: phsr@if.ufrj.br

is conserved through the entire evolution. Thus, this restricts the way the populations (in the referred basis) are transferred. Here \hat{n}_S and \hat{n}_R are the excitation-number operators of the system S and R respectively. For the specific case in which S represents a two level atom interacting with one mode of the electromagnetic field in a cavity, these operators are given by $\hat{n}_S = \frac{1}{2}(\mathbb{I} - \sigma_z)$ and $\hat{n}_R = \hat{a}^\dagger \hat{a}$. The conservation of $\langle \hat{N} \rangle$ follows immediately from the expressions for $\langle \hat{n}_R(p) \rangle$ and $\langle \hat{n}_S(p) \rangle$,

$$\begin{aligned}\langle \hat{n}_S(p) \rangle &= \text{Tr}[\rho_S(p)\hat{n}_S] = \rho_{ee}(1-p), \\ \langle \hat{n}_R(p) \rangle &= \text{Tr}[\rho_R(p)\hat{n}_R] = \rho_{ee}p,\end{aligned}\quad (6)$$

so that $\langle \hat{N} \rangle = \rho_{ee}$.

In the following, we investigate how the conservation (5) manifests itself in the evolution of the purity $\pi_i \equiv \text{Tr}\rho_i^2$ of the subsystem $i = S, R$. With the aid of Eqs. (4) and (6) it is straightforward to show that $\pi_i(p)$ can be written as

$$\pi_i(p) = 2 \langle \hat{n}_i(p) \rangle^2 - 2 \langle \hat{n}_i(p) \rangle \Lambda + 1, \quad (7)$$

where $\Lambda = 1 - |\rho_{ge}|^2 / \rho_{ee}$. Inverting this expression, we obtain

$$\langle \hat{n}_i(p) \rangle = \frac{\Lambda}{2} \pm \frac{1}{2} \sqrt{\Lambda^2 - 2(1 - \pi_i(p))}. \quad (8)$$

Hence we can rewrite the conservation equation (5) as

$$\rho_{ee} = \Lambda \pm \mathcal{W}_S(\Lambda, p) \pm \mathcal{W}_R(\Lambda, p), \quad (9)$$

where we have defined $\mathcal{W}_i(\Lambda, p) = \frac{1}{2} \sqrt{\Lambda^2 - 2(1 - \pi_i(p))}$. As seen in Eq. (8), the appropriate choice of the sign in front of \mathcal{W}_i depends on whether $\langle \hat{n}_i(p) \rangle$ is greater or smaller than $\Lambda/2$. If the initial value ρ_{ee} is smaller than or equal to $\Lambda/2$, then the restriction $\langle \hat{n}_i(p) \rangle \leq \rho_{ee}$ implies that $\langle \hat{n}_i(p) \rangle \leq \Lambda/2$, and both minus signs should be taken in (9). On the other hand, if ρ_{ee} is larger than $\Lambda/2$, then the signs in (9) depend on the value of p . From Eqs. (6) it follows that $\langle \hat{n}_S(p) \rangle \geq \Lambda/2$ whenever $p \leq 1 - \Lambda/2\rho_{ee}$, whereas $\langle \hat{n}_R(p) \rangle \geq \Lambda/2$ for every $p \geq \Lambda/2\rho_{ee}$. In both cases the upper/lower inequality sign determine the \pm sign that should be used.

With the previous results we see that as a consequence of the conservation of $\langle \hat{N} \rangle$, the purities $\pi_S(p)$ and $\pi_R(p)$ evolve in such a way that the right hand side of Eq. (9) – or more generally any function of this argument – remains constant during the evolution.

Entanglement conservation. We recognized that a dynamical invariance property of the map (3) can be used to reveal that more complex quantities (in this case the purity of each subsystem) can be combined into new invariant forms. The purity of a system provides a different physical content from the excitation number, and this is the starting point for the following analysis. If the quantum state ρ_S has purity different from one, then there exists a larger system in a pure state, so that the reduced density operator corresponding to S is precisely the mixed state ρ_S . We will refer to the system needed to purify the enlarged system as M . The recognition of this

latter system is crucial, not only for the understanding of the physical origin of states such as $\rho_S(0)$, but also because it throws some light into the global dynamical properties of (bipartite) entanglement for systems undergoing the interaction modeled by (3).

Let us suppose that $\rho_S(0)$ results from partial tracing over the system M on the pure general state

$$|\psi(0)\rangle = \alpha |M_1\rangle|e\rangle + \beta |M_0\rangle|g\rangle + \gamma |M_1\rangle|g\rangle + \delta |M_0\rangle|e\rangle, \quad (10)$$

where $|M_0\rangle, |M_1\rangle$ are two orthogonal states of M . In this case the elements of the initial density matrix $\rho_S(0)$ are $\rho_{ee} = |\alpha|^2 + |\delta|^2$, $\rho_{ge} = \beta\delta^* + \alpha^*\gamma$, and $\rho_{gg} = |\beta|^2 + |\gamma|^2$. At $t = 0$ we allow system S to interact with the environment, according to the transformation (3). Then, the initial tripartite state $|\Psi(0)\rangle = |\psi(0)\rangle |\phi_0\rangle$ evolves to

$$\begin{aligned}|\Psi(p)\rangle &= \alpha |M_1\rangle(\sqrt{1-p}|e\rangle|\phi_0\rangle + \sqrt{p}|g\rangle|\phi_1\rangle) + \\ &+ \delta |M_0\rangle(\sqrt{1-p}|e\rangle|\phi_0\rangle + \sqrt{p}|g\rangle|\phi_1\rangle) + \\ &+ (\beta |M_0\rangle + \gamma |M_1\rangle)|g\rangle|\phi_0\rangle.\end{aligned}\quad (11)$$

Using (11), the density matrix $\rho_{MSR}(p)$ of the complete system may be constructed, and the reduced density matrices $\rho_i(p)$ with $i = M, R, S$ can be computed. Since M does not interact at all ρ_M is constant and given by

$$\rho_M = \begin{pmatrix} |\beta|^2 + |\delta|^2 & \beta\gamma^* + \alpha^*\delta \\ \alpha\delta^* + \beta^*\gamma & |\alpha|^2 + |\gamma|^2 \end{pmatrix}. \quad (12)$$

We return to Eq. (9) and observe that, given it was obtained from a property of the interaction between R and S only, it remains valid once the system M has been considered. Moreover, as seen from Eq. (11), the coefficients (α and δ) that determine ρ_{ee} are precisely the coefficients responsible for the entanglement between M and the rest of the system. This is an important observation since it relates ρ_{ee} directly to such entanglement, and hence allows us to relate ρ_{ee} with the (constant) purity of the system M as follows

$$\begin{aligned}\rho_{ee} &= \frac{\Lambda}{2} \pm \frac{1}{2} \sqrt{\Lambda^2 - 2(1 - \pi_M)} \\ &= \frac{\Lambda}{2} \pm \mathcal{W}_M(\Lambda).\end{aligned}\quad (13)$$

Once more, the \pm sign depends on whether ρ_{ee} is larger (plus sign) or smaller (minus sign) than $\Lambda/2$. Introducing this last expression into Eq. (9) leads to

$$\pm \mathcal{W}_M(\Lambda) - \frac{\Lambda}{2} = \pm \mathcal{W}_S(\Lambda, p) \pm \mathcal{W}_R(\Lambda, p). \quad (14)$$

As has been stated above, the appropriate choice of signs for each \mathcal{W}_i is determined by the magnitude of ρ_{ee} relative to $\Lambda/2$, as well as by the value of p . An inspection of all the valid combinations leads finally to the following cases (we omit the dependence on Λ):

$$\frac{\Lambda}{2} + \mathcal{W}_M = \mathcal{W}_S(p) + \mathcal{W}_R(p), \quad p \in [0, 1], \quad (15)$$

whenever $\rho_{ee} \leq \frac{\Lambda}{2}$, and

$$\frac{\Lambda}{2} - \mathcal{W}_M = \begin{cases} \mathcal{W}_R(p) - \mathcal{W}_S(p), & p < 1 - \frac{\Lambda}{2\rho_{ee}} \\ \mathcal{W}_S(p) + \mathcal{W}_R(p), & p \in [1 - \frac{\Lambda}{2\rho_{ee}}, \frac{\Lambda}{2\rho_{ee}}] \\ \mathcal{W}_S(p) - \mathcal{W}_R(p), & p > \frac{\Lambda}{2\rho_{ee}}, \end{cases} \quad (16)$$

whenever $\rho_{ee} > \frac{\Lambda}{2}$.

Since the tripartite state remains pure during the evolution, each π_i may be regarded as a quantitative measure of bipartite entanglement between system i and the rest. Alternatively, we may use a measure based on the Schmidt weight K_i [17], which are related to π_i according to $\pi_i(p) = K_i^{-1}(p)$. As a result, Eqs. (15)-(16) stand as conservation relations for bipartite entanglement. We conclude that, once the original S - R system is enlarged to include system M needed for purification, the conservation law (5) acquires a new significance in terms of conservation of bipartite entanglement. The initial entanglement between S and M turns into entanglement between M and R , and the entanglement transfer is described by Eqs. (15)-(16).

In the particular case in which the initial density matrix $\rho_S(0)$ is diagonal so that $\Lambda = 1$ (for example if $\delta = \gamma = 0$ in Eq. (10)), then the conservation relations (15)-(16) involve the quantities $W_i(p) \equiv \mathcal{W}_i(1, p) = \sqrt{\frac{1}{2K_i(p)} - \frac{1}{4}}$, which are explicitly written as

$$\begin{aligned} W_S(p) &= |\rho_{ee}(1-p) - \frac{1}{2}|, \\ W_R(p) &= |\rho_{ee}p - \frac{1}{2}|, \\ W_M &= |\rho_{ee} - \frac{1}{2}|, \end{aligned} \quad (17)$$

as follows from the definition of W_i and Eqs. (6)-(7).

The conservation relations (15)-(16) for $\Lambda = 1$ hold even when we consider system M to be in an initial state entangled with N qubits S_j ($j = 1, 2, \dots, N$). This allows us to find new global quantities that are conserved during the evolution. For example, the expression equivalent to Eq. (15) for the $N + 1$ GHZ-type state

$$|\chi_N\rangle = \alpha |M_1\rangle \Pi_j^N |e_j\rangle + \beta |M_0\rangle \Pi_j^N |g_j\rangle \quad (18)$$

is:

$$W_M + \frac{1}{2} = \frac{1}{N} \sum_{j=1}^N [W_{S_j}(p_j) + W_{R_j}(p_j)]. \quad (19)$$

Experimental realization. We verified the validity of Eqs. (15) and (16) using polarization-entangled photons generated from spontaneous parametric down conversion (SPDC). The polarization entanglement is prepared with a two-crystal source [18]. The experimental setup is shown in figure 1. A 325nm cw He-Cd laser is used to pump two 1mm long type-I BBO crystals. The down-converted photons are spectrally filtered with 10nm bandwidth interference filters, and spatially filtered through 2mm detection apertures, before detection with single-photon counting modules. Identifying

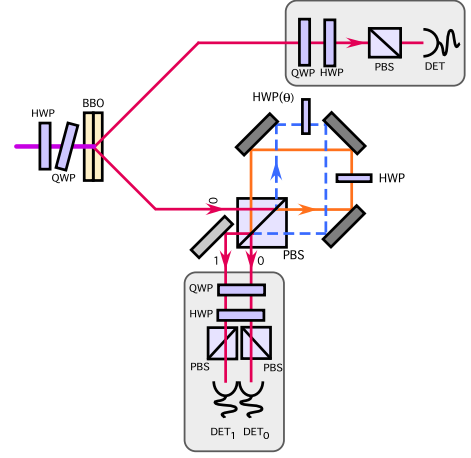


FIG. 1: Experimental setup.

the polarization state of photon 2 as the system S and the polarization state of photon 1 as the third party M , the source is set up to produce the initial state

$$|\Phi\rangle = \alpha |V\rangle_M |V\rangle_S + \beta |H\rangle_M |H\rangle_S.$$

Let us further identify the longitudinal spatial mode of photon 2 as the reservoir R , and call the initial spatial mode $|0\rangle$. A displaced Sagnac interferometer with a nested wave-plate can be used to implement the following transformation on the polarization and spatial mode of photon 1 [11, 13, 14]

$$\begin{aligned} |H\rangle |0\rangle &\rightarrow |H\rangle |0\rangle, \\ |V\rangle |0\rangle &\rightarrow \cos\theta |V\rangle |0\rangle + \sin\theta |H\rangle |1\rangle, \end{aligned} \quad (20)$$

where $|0\rangle$ and $|1\rangle$ refer to different spatial modes and θ is twice the angle of the half-wave plate. It has been demonstrated with quantum process tomography that this interferometer implements the amplitude damping channel with fidelities as high as ~ 0.95 [14]. Identifying the polarization states $\{|H\rangle, |V\rangle\}$ with the system states $\{|g\rangle, |e\rangle\}$, the spatial modes $\{|0\rangle, |1\rangle\}$ with the reservoir states $\{|\phi_0\rangle, |\phi_1\rangle\}$, and $p = \sin^2\theta$, the transformation (20) becomes equivalent to (3), provided $0 \leq \theta \leq \pi/2$. The initial state $|\Psi\rangle_{SM} |0\rangle_R$ evolves to

$$\begin{aligned} |\Phi(\theta)\rangle &= \beta |H\rangle_M |H\rangle_S + \alpha \cos\theta |V\rangle_M |V\rangle_S |0\rangle_R \\ &\quad + \alpha \sin\theta |V\rangle_M |H\rangle_S |1\rangle_R, \end{aligned} \quad (21)$$

after propagation through the interferometer. The final state is equivalent to $|\Psi(p)\rangle$ given in equation (11) with $\gamma = \delta = 0$. It is important to note that partially tracing over any two of the three subsystems of the state (21) leads to a diagonal reduced density matrix. Then, the purities π_j (or equivalently, the Schmidt weights K_j) and each W_j ($j = S, M, R$) term in Eq. (15) can be determined by local population measurements, made with the detectors 0 and 1 shown in Fig. (1).

By rotating the half-wave plate (HWP) in the pump beam, we selected different values of α and β . For instance, we selected $|\alpha|^2 = \rho_{ee} = 0.31, 0.5, 0.73$ with corresponding purities 0.97, 0.94 and 0.96, so that the conservation laws could be

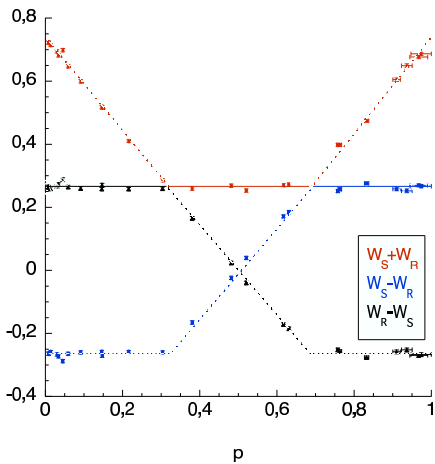


FIG. 2: Experimental results for $\rho_{ee} = 0.73$, $\Lambda = 1$. The coloured lines correspond to the functions $W_R(p) - W_S(p)$ (black), $W_S(p) + W_R(p)$ (red) and $W_S(p) - W_R(p)$ (blue). The continuous line represents the invariant I_{SR} .

applied directly. These purities were calculated from quantum state tomography of the initial states (after passage through the interferometer with $\theta = 0$, see below). Imperfect purity is probably due to spatial walk-off in the crystal and imperfect alignment of the interferometer. These parameters indicate that the experimental state is quite close to the ideal initial pure state.

Projective measurements on S and M are performed using wave-plates and polarizing beam splitters to project onto polarization states, while projection onto spatial modes is performed by placing detectors in mode 0 or 1. We performed measurements for several values of $p = \sin^2 \theta$ ($0 \leq \theta \leq \pi/2$) characterizing the amplitude damping channel in (20).

Figure 2 shows the theoretical curves and the experimental data of each of the three functions that define the invariant $I_{SR} = \frac{\Lambda}{2} - \mathcal{W}_M$, according to Eq. (16) for the case $\rho_{ee} = 0.73$ and $\Lambda = 1$. The black curve corresponds to

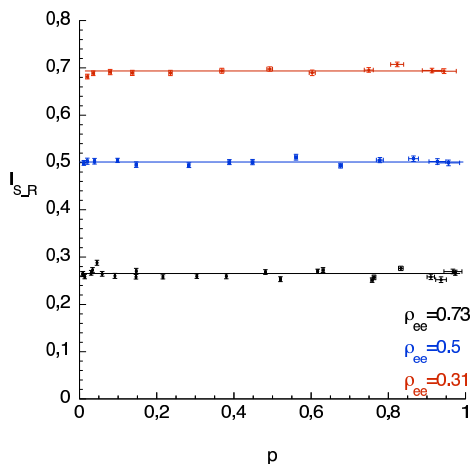


FIG. 3: The invariant I_{SR} for different values of ρ_{ee}

$W_R(p) - W_S(p)$, the red one to $W_S(p) + W_R(p)$, and the blue one to $W_S(p) - W_R(p)$. The invariant (piecewise) function I_{SR} is here stressed by the continuous line and corresponds, as follows from Eq. (16) (with $\Lambda = 1$), to one of the above curves depending on whether p is in the interval $\left[0, 1 - \frac{1}{2\rho_{ee}}\right)$, $\left[1 - \frac{1}{2\rho_{ee}}, \frac{1}{2\rho_{ee}}\right]$ or $\left(\frac{1}{2\rho_{ee}}, 1\right]$.

Figure 3 shows both the theoretical and experimental curves of the invariant quantity I_{SR} for three different values of ρ_{ee} (in all cases $\Lambda = 1$). The red and blue curves, corresponding respectively to $\rho_{ee} = 0.31$ and $\rho_{ee} = 0.5$, represent the invariant sum $I_{SR} = \frac{1}{2} + \mathcal{W}_M = W_S(p) + W_R(p)$ (see Eq. (15)), whereas the black curve, corresponding to $\rho_{ee} = 0.73$, represents the invariant $I_{SR} = \frac{1}{2} - \mathcal{W}_M$ given by the expression (16). From figures 2 and 3 we see that the experimental data fit the theoretical curves within the precision of the measurements, thus demonstrating experimentally the conservation relations (15)-(16).

In conclusion, we showed that by adding a third party in the interaction between two two-level systems, it is possible to obtain quantities that are invariants in the evolution of the entanglement. We performed an experimental demonstration of the process using entangled photons and verified the invariance of these quantities.

The authors acknowledge the Brazilian funding agencies CNPq, CAPES and FAPERJ. This work is part of the National Institute for Science and Technology for Quantum Information, and it was supported in the US by DARPA HR0011-09-1-0008 and ARO W911NF-09-1-0385. A.V.H. and O.J.F were funded by the Consejo Nacional de Ciencia y Tecnología, México.

-
- [1] K. Życzkowski, P. Horodecki, M. Horodecki, and R. Horodecki, Phys. Rev. A **65**, 012101 (2001).
 - [2] C. Simon and J. Kempe, Phys. Rev. A **65**, 052327 (2002).
 - [3] L. Diósi, Progressive decoherence and total environmental disentanglement, in *Irreversible Quantum Dynamics*, edited by F. Benatti and R. Floreanini, pp. 157–163, Springer, Berlin, 2003.
 - [4] P. J. Dodd and J. J. Halliwell, Phys. Rev. A **69**, 052105 (2004).
 - [5] W. Dür and H.-J. Briegel, Phys. Rev. Lett. **92**, 180403 (2004).
 - [6] T. Yu and J. H. Eberly, Phys. Rev. Lett. **93**, 140404 (2004).
 - [7] F. Mintert, A. R. R. Carvalho, M. Kuś, and A. Buchleitner, Phys. Rep. **415**, 207 (2005).
 - [8] M. Hein, W. Dür, and H.-J. Briegel, Phys. Rev. A **71**, 032350 (2005).
 - [9] M. F. Santos, P. Milman, L. Davidovich, and N. Zagury, Phys. Rev. A **73**, 040305 (2006).
 - [10] T. Yu and J. H. Eberly, Phys. Rev. Lett. **97**, 140403 (2006), Science **323**, 598 (2009).
 - [11] M. P. Almeida *et al.*, Science **316**, 579 (2007).
 - [12] A. R. R. Carvalho, F. Mintert, S. Palzer, and A. Buchleitner, Eur. Phys. J. D **41**, 425 (2007).
 - [13] A. Salles *et al.*, Phys. Rev. A **78**, 022322 (2008).
 - [14] O. J. Farias, C. L. Latune, S. P. Walborn, L. Davidovich, and P. H. S. Ribeiro, Science **324**, 1414 (2009).

- [15] M. L. Aolita, R. Chaves, D. Cavalcanti, A. Acín, and L. Davidovich, *Phys. Rev. Lett.* **100**, 080501 (2008).
- [16] D. Bouwmeester, A. Ekert, and A. Zeilinger, editors, *The Physics of Quantum Information* (Springer Verlag, Berlin, 2000).
- [17] See, e.g., X.F. Qian and J.H. Eberly, for a discussion in arXiv:1009.5622 (2010).
- [18] P. G. Kwiat, E. Waks, A. G. White, I. Appelbaum, and P. H. Eberhard, *Phys. Rev. A.* **60**, R773 (1999).